

## Influence of Room-Temperature-Stretching Technology on the Crystalline Morphology and Microstructure of PVDF Hard Elastic Film

Caihong Lei, Bing Hu, Ruijie Xu, Qi Cai, Wenqiang Shi

Department of Polymer Materials Science and Engineering, School of Materials and Energy, Guangdong University of Technology, Guangzhou 510006, China

Correspondence to: C. Lei (E-mail: Lch528@gdut.edu.cn)

**ABSTRACT:** The crystalline morphology and microstructure during stretching of polyvinylidene fluoride hard elastic film under room temperature was followed using wide-angle X-ray diffraction (WAXD), differential scanning calorimetry (DSC), and scanning electron microscopy (SEM). It was found that an endotherm plateau from the contribution of some new crystals formed during annealing appeared and some thinner lamellae existed in the annealed film. During stretching, the endotherm plateau disappeared and those thinner lamellae transformed into  $\beta$ -phase. At the same time, some initial pores were observed. With increasing stretching ratio from 20 to 100%, the  $\beta$ -phase content increased, whereas within the strain rate range of 0.003–0.034 s<sup>-1</sup>, its content was least under 0.017 s<sup>-1</sup>. During stretching, lamellae separation, crystalline morphology transformation and disappearance of grown crystals formed by annealing coexisted. From the viewpoint of pore initiation, less crystalline morphology transformation was beneficial for the lamellae separation. Higher stretching ratio resulted in the breakage of separated lamellae. © 2013 Wiley Periodicals, Inc. *J. Appl. Polym. Sci.* **2014**, *131*, 40077.

**KEYWORDS:** membranes; morphology; properties and characterization

Received 2 August 2013; accepted 20 October 2013

DOI: 10.1002/app.40077

### INTRODUCTION

Because of its excellent chemical inertness and good physical and thermal stability, polyvinylidene fluoride (PVDF) as a material has attracted a great interest in the membrane industry.<sup>1–4</sup> Normally, PVDF microporous membrane can be prepared based on phase inversion process<sup>5</sup> and thermal-induced phase separation.<sup>6</sup> Compared with these two methods, melt-stretching method has the advantages such as no solvent usage and less environmental pollution, which has been successfully used to fabricate polypropylene and polyethylene microporous membranes.<sup>7,8</sup>

Using melt-spinning and stretching method, PVDF hollow fiber membrane was prepared by Du,<sup>9</sup> where the samples were firstly annealed under 140°C for 30 min and then stretched to a ratio of 10–30% under room temperature, followed by a hot stretch with 120% ratio under 80°C. Sadeghi<sup>10</sup> prepared PVDF microporous membrane using cast extrusion and stretching technology, where cold stretching to 35% strain at room temperature and hot stretching to 55% at 120°C under the same speed of 50 mm min<sup>-1</sup> were applied. However, it is still unclear what have happened during stretching and if there is any relationship between the crystalline morphology transformation and pore formation.

As to the crystalline morphology transformation, many works have proved that when films of PVDF  $\alpha$ -phase are mechanically

stretched or drawn to a certain percent elongation at a given temperature, the nonpolar crystalline  $\alpha$ -phase converts into the polar  $\beta$ -phase and the  $\beta/\alpha$  ratios are affected by stretching temperature, rate and ratio.<sup>11</sup> It is already known that stretching at higher strain rates will result in a more efficient  $\alpha$ - $\beta$  transformation,<sup>12</sup> which is due to that at a higher stretching rate the relaxation of stress occurring during stretching is lower. As to the stretching ratio, drawing above 4 brings about the  $\alpha$  to  $\beta$  crystalline phase transformation. Gregorio<sup>13</sup> reported that stretching at temperatures around 80°C yielded the maximum conversion to the  $\beta$ -phase. AndreÇ-Castagnet<sup>14</sup> found that during stretching below 100°C, the forces could be transmitted on crystalline lamellae, yielding fragmentation and phase transformation from  $\alpha$ -phase to  $\beta$ -phase. At higher temperatures, polymer chains became more mobile and therefore there was less conversion. Sencadas<sup>15</sup> also reported that the maximum  $\beta$ -phase content was achieved at 80°C with a stretching ratio of 5.

For stretched PVDF fibers, Mohammadi<sup>16</sup> has found that the  $\beta$ -phase content had an abrupt increase when stretched near 70°C, and then it decreased with increasing stretching temperature. The highest content of well oriented  $\beta$ -phase, 86.5%, was achieved during drawing at 50 mm min<sup>-1</sup>. Matsushige<sup>17</sup> reported that for the samples stretched at lower temperatures, the crystal transformation occurred at the region where necking

was initiated. Wu<sup>18</sup> also found that the alternating necked and unnecked regions were aligned along the fibers and in necked regions more  $\alpha$  to  $\beta$  phase transformation took place than in unnecked regions.

Normally there are three consecutive stages to fabricate microporous membrane based on melt-stretching mechanism: (1) production of the precursor film with a lamellar morphology, (2) annealing of the film to thicken the lamellae, and (3) stretching of the film at low temperature to create voids and then stretching at high temperature to enlarge pores. According to Johnson,<sup>19</sup> the microvoid morphologies were a consequence of interlamellar separation. Sadeghi<sup>20</sup> summarized that the following phenomena took place simultaneously during cold-stretching: (1) void formation as a result of chain scission of short tie chains, (2) slippage of crystal blocks and their reorientation along the stretching direction, (3) stretching of longer tie chains as shorter tie chains were broken apart, and (4) crystallization of highly stretched long tie chains. In our previous work,<sup>21,22</sup> we have found that during stretching polypropylene hard elastomer under room temperature, the low temperature endotherm plateau in the differential scanning calorimetry curves and the plastic plateau in the stress-strain curves, which were formed during annealing, disappeared progressively and their disappearance corresponded to the formation of bridge structure connecting separated lamellae.

Compared with that of polypropylene microporous membrane, the preparation of PVDF microporous membrane becomes difficult and complex, due to the existence of crystalline morphology transformation during stretching. Therefore, it is necessary to make it clear about the crystalline morphology transformation and pore initiation during room temperature stretching. In this article, the annealed PVDF film with elastic recovery of 91.5% was stretched under room temperature. The influence of strain rate and ratio on the crystalline morphology and microstructure was investigated.

## EXPERIMENTAL

### Materials

Extrusion grade PVDF (solef 1010) was supplied by Solvay (Tavaux, France). The melt flow index was 2 g/10 min (230°C, 2.16 kg load). The melting peak point ( $T_m$ ) and crystallinity, obtained from differential scanning calorimetry (DSC; PerkinElmer DSC 7, MA) at a rate of 10°C min<sup>-1</sup>, were 171°C and 43.0%.

### Precursor and Cold-Stretched Film Preparation

The cast film was prepared by cast extrusion through a T-slot die followed by stretching and thermal-setting. During extrusion, the uniaxial (machine direction, MD) stretching was applied to PVDF melt, which resulted in the oriented crystalline structures. The die temperature was set at 240°C and the melt-draw ratio was set at 64. The films were produced under chill roll temperature of 90°C and the obtained films had a thickness of 40  $\mu$ m. The prepared precursor film was then annealed at taut condition for 2 h at 145°C. The stretching of the annealed film was taken using an Instron 5500R machine equipped with a heating chamber. The annealed films were stretched under

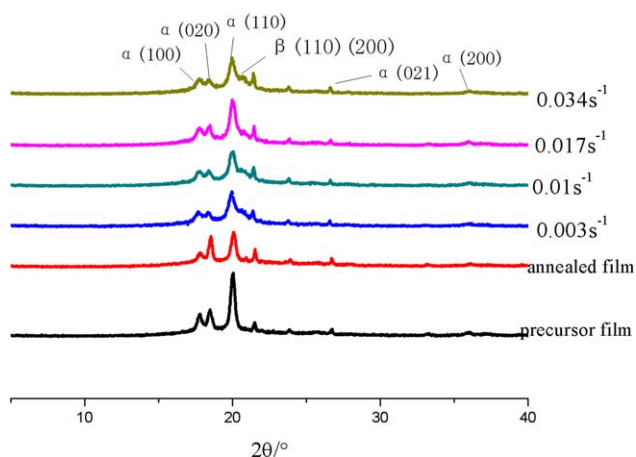


**Figure 1.** WAXD curves of PVDF film stretched to 60% under different rates. [Color figure can be viewed in the online issue, which is available at [wileyonlinelibrary.com](http://wileyonlinelibrary.com).]

room temperature to 20, 40, 60, 80, and 100%, respectively, at a strain rate of 0.017 s<sup>-1</sup>. Also the annealed films were stretched to 60% under different rate. After stretching, all the films were heat-set under 145°C for 5 min in order to avoid shrinkage of the stretched samples after removing the cold stretching load.

### Characterization

The engineering stress-strain curve of annealed film was tested using Instron 5500R machine at a strain rate of 0.017 s<sup>-1</sup>. The original length of the sample between the Instron clamps was 50 mm. The true strain is defined as  $\varepsilon = (L - L_0)/L_0$ , where  $L$  is the extended length and  $L_0$  is the initial length. Assuming the volume keeps constant in the drawing process, the true stress can be calculated by the following relation:  $\sigma_f = \sigma \times (1 + \varepsilon)$ , where  $\sigma$  is the engineering stress.

The thermal behavior was observed using a differential scanning calorimeter (Perkin-Elmer DSC-7, PerkinElmer). The samples of about 5 mg were cut from the central area of deformed films. The cell constant calibration was performed with an indium standard, and the temperature calibration was obtained with indium and lead metals. The temperature was raised from 50 to 200°C at a rate of 5°C min<sup>-1</sup> in a nitrogen atmosphere.

The wide-angle X-ray diffraction (WAXD) measurements were carried out using a Bruker AXS X-ray goniometer (Karlsruhe, Germany). The generator was set up at 40 kV and 40 mA and the copper Cu K $\alpha$  radiation was selected using a graphite crystal monochromator. The sample to detector distance was fixed at 8 cm.

Surface morphology was characterized by scanning electron microscopy (SEM, S3400, Hitachi, Japan). All the samples were sputtered with a platinum ion beam for 300 s before test.

## RESULTS AND DISCUSSION

### Crystalline Morphology and Microstructure under Different Room-temperature Strain Rates

To study the crystalline morphology of PVDF films stretched under different strain rates, the WAXD testing was carried out. Figure 1 gives the WAXD curves of film stretched to 60% under

**Table I.** The Content of  $\beta$ -phase under Different Strain Rates

Strain rate ( $s^{-1}$ )	0.003	0.01	0.017	0.034
$\beta$ -phase content (%)	39.8	33.6	9.8	26.3

different rates. The peaks at diffraction angles of  $17.8^\circ$ ,  $18.4^\circ$ ,  $20.0^\circ$ ,  $26.7^\circ$ ,  $33.2^\circ$ , and  $36.0^\circ$  correspond to (100), (020), (110), (021), (130), and (200) crystal plane of  $\alpha$ -phase.<sup>10</sup> It can be seen for the precursor and annealed film, only  $\alpha$ -phase exists. After stretching, a new weak peak at  $20.7^\circ$  appears. It is known that the  $\beta$ -phase has only a prominent peak at  $20.7^\circ$  in the WAXD spectrum attributed to (110/200) planes.<sup>23</sup> The WAXD curves indicate that some content of  $\beta$ -phase is formed and stretching induces the transformation from  $\alpha$ -phase to  $\beta$ -phase. Using origin peak separation software, the  $\beta$ -phase content was obtained by calculating the ratio of the crystallinity of  $\beta$  to  $\alpha$  phase and listed in Table I. The results in Table I indicate that with increasing strain rate from 0.003 to  $0.017 s^{-1}$ , the content decreases and then increases again under  $0.034 s^{-1}$ . This means that under appropriate rate around  $0.017 s^{-1}$ , the transformation from  $\alpha$  to  $\beta$ -phase is least. This is in contrary to those results from other papers,<sup>12,24</sup> where higher strain rate leads to higher transformation.

Figure 2 gives DSC curves of PVDF film stretched to 60% under different rates. Compared with that of precursor film, after annealing, the pronounced change is the appearance of a low temperature endotherm plateau around  $145^\circ C$ . This is similar to that in annealed polypropylene films.<sup>21,22</sup> Sang-Young Lee<sup>25</sup> proposed that at higher annealing temperatures, some loose tie chain segments probably evolved into crystallites. In our previous work,<sup>21</sup> the plateau existence was attributed to some crystallization behavior occurrence around initial lamellar structure. In annealed PVDF fibers, Li attributed it to secondary crystallization.<sup>26</sup> In their view, secondary crystallization corresponded to the progressive formation of a population of unstable crystals. Under  $0.003 s^{-1}$ , it is apparent that the endotherm plateau around  $145^\circ C$  still exists, but it disappears under higher strain rates. Similar phenomenon has been observed in stretch-

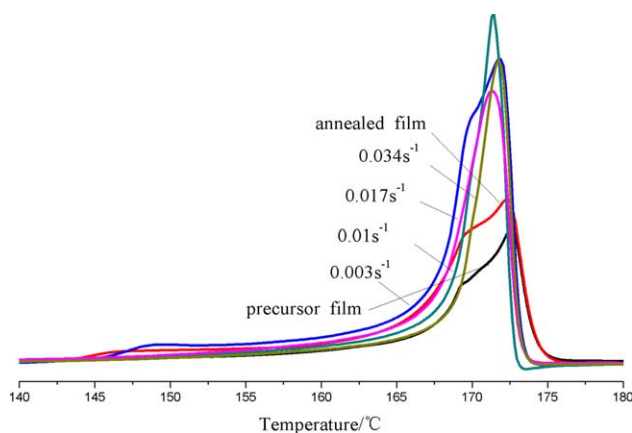


**Figure 2.** DSC curves of PVDF film stretched to 60% under different rates. [Color figure can be viewed in the online issue, which is available at [wileyonlinelibrary.com](http://wileyonlinelibrary.com).]

ing of annealed polypropylene film under room temperature.<sup>21</sup> The plateau disappearance is related with the lamellae separation and corresponds to the formation of initial bridge structure connecting separated lamellae. The plateau existence under  $0.003 s^{-1}$  means that this lower strain rate is not enough to make the initial lamellae separated. In Table I, the  $\beta$ -phase content under  $0.003 s^{-1}$  is maximum and decreases with increasing strain rate to  $0.017 s^{-1}$ . Hence, it can be deduced that the endotherm plateau does not transform to  $\beta$ -phase during stretching.

In addition, in Figure 2 there is a weak shoulder around  $169^\circ C$  for precursor and annealed film. In Sadeghi's work,<sup>10</sup> for PVDF with low molecular weight, a small shoulder was also seen at lower temperature. They attributed it to two close lamellae thickness distributions. The above WAXD results prove that there is no  $\beta$ -phase in the annealed film. Therefore, the small shoulder can not come from the  $\beta$ -phase. After stretching under higher strain rates, the shoulder disappears. The disappearance of the small shoulder in annealed film during stretching indicates that some blocks of lamellae are torn away from the initial lamellae. Hence, the weak shoulder in annealed film may be from some thinner lamellae formed by stress-induced crystallization during cast extrusion. Combined with the appearance of  $\beta$ -phase after stretching, it is deduced that these weak crystals reorganize and recrystallize to form  $\beta$ -phase during stretching. Similar view has been proposed by Du<sup>27</sup> and they attributed the phase transformation to the reorganization of some imperfect crystals existing among the lamellae. To our surprise, after stretching under  $0.003 s^{-1}$ , there is also a shoulder around  $169^\circ C$ , similar to that in annealed film. This may be from the contribution of higher  $\beta$ -phase content under this strain rate. As to the melting point of  $\alpha$ -phase and  $\beta$ -phase of PVDF, there are different views in the related works.<sup>11,14,28</sup> The highest  $\beta$ -phase cell density provides more packing and higher melting temperature crystals.<sup>26</sup> But Satapathy et al.<sup>14,28</sup> found that the melting point of  $\beta$ -phase is less than that of  $\alpha$ -phase. In the sample stretched under  $0.003 s^{-1}$ , the shoulder temperature is around  $169^\circ C$  and the main peak temperature is around  $171^\circ C$ . Under other strain rates, the peak temperatures are around  $171^\circ C$ . The above WAXD result under  $0.017 s^{-1}$  shows that the sample is mainly composed of  $\alpha$ -phase. Hence, the peak around  $171^\circ C$  is from the  $\alpha$ -phase. With increasing  $\beta$ -phase content, the melting peak from  $\beta$ -phase becomes pronounced, leading to the appearance of shoulder around  $169^\circ C$  for sample stretched under  $0.003 s^{-1}$ .

Figure 3 shows SEM of PVDF film stretched to 60% under different rates. Under  $0.003 s^{-1}$ , it is apparent that the lamellae separation behavior is worse, in agreement with the above DSC result. Under 0.01 and  $0.017 s^{-1}$ , apparent pore structure can be seen. Further increase the strain rate to  $0.034 s^{-1}$  leads to some cracks appearance. Also with increasing strain rate, lamellae deformation becomes pronounced. Contrary to that in stretched polypropylene film,<sup>21</sup> no apparent connecting bridges can be observed, although some pores have been initiated.

It can be seen that during stretching of annealed PVDF film, the lamellae separation and the transformation of thinner

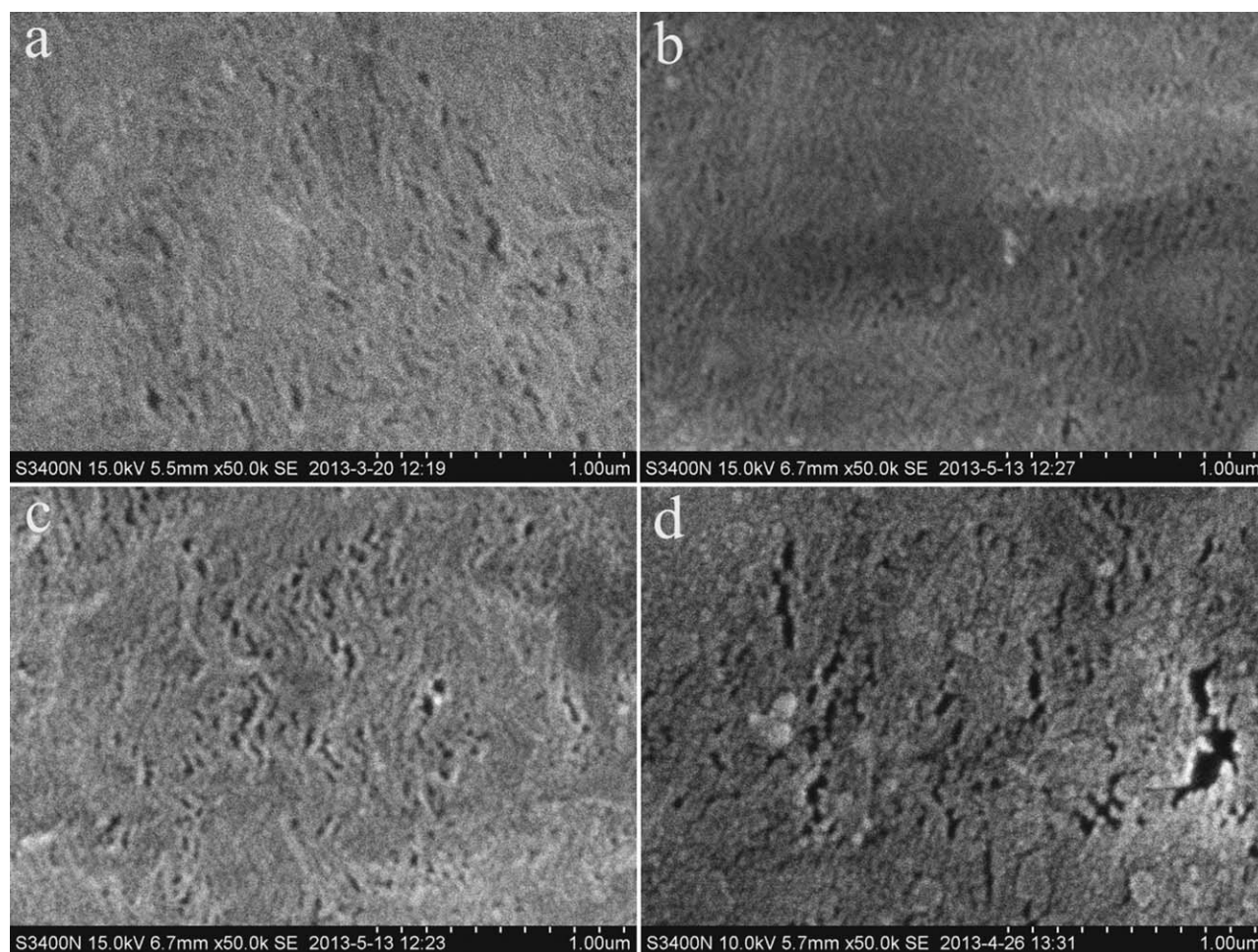


**Figure 3.** SEM of PVDF film stretched under room temperature with different rates, (a)  $0.003 \text{ s}^{-1}$ , (b)  $0.01 \text{ s}^{-1}$ , (c)  $0.017 \text{ s}^{-1}$ , (d)  $0.034 \text{ s}^{-1}$ .

crystals to  $\beta$ -phase coexist. At lower strain rate, the lamellae separation is not good and the lower rate is not enough to induce the disappearance of endotherm plateau. At this time more stress is used to transform the thinner crystals, resulting in higher content of  $\beta$ -phase. With increasing strain rate to  $0.017 \text{ s}^{-1}$ , more stress is used to separate lamellae and better lamellae separation is obtained, whereas  $\beta$ -phase content is least. The formation of initial pore structure competes with the crystalline transformation. At a faster strain rate such as  $0.034 \text{ s}^{-1}$ , the degree of fragmentation and reorganization of thinner crystals induced by stress is large enough to cause a higher  $\beta$ -phase transformation. At the same time lamellae deformation and breakage are inevitable.

#### Crystalline Morphology and Microstructure under Different Stretching Ratios

Figure 4 gives true stress–strain curve of annealed PVDF film under room temperature at a strain rate of  $0.017 \text{ s}^{-1}$ . No typical necking phenomenon can be observed. After the initial elastic region, a plastic plateau is followed. Then pronounced strain-hardening behavior is seen. The film shows typical hard elastic behavior. The elastic recovery when stretched to 80% is up to 91.5%. To follow the crystalline morphology and microstructure change during stretching

under room temperature, the films with strain ratio of 20, 40, 60, 80, and 100%, respectively, were prepared.

Figure 5 gives the WAXD curves of PVDF film stretched to different ratios. Compared with that of annealed film, new peak

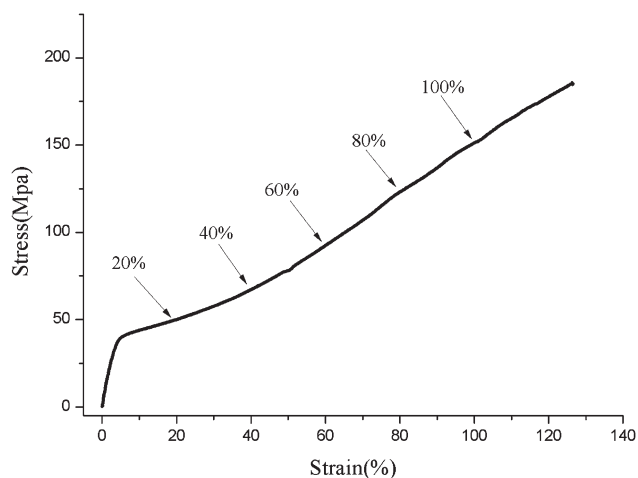


**Figure 4.** Stress–strain curve of annealed PVDF film under strain rate of  $0.017 \text{ s}^{-1}$ .

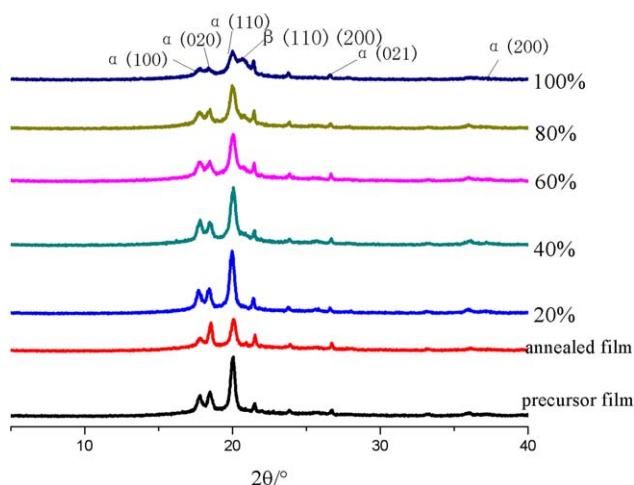


**Figure 5.** WAXD curves of PVDF film stretched to different ratios under room temperature. [Color figure can be viewed in the online issue, which is available at [wileyonlinelibrary.com](http://wileyonlinelibrary.com).]

appears around  $20.7^\circ$  from the contribution of (110) and (200) plane of  $\beta$ -phase. Using origin peak separation software, the  $\beta$ -phase content was obtained and listed in Table II. The content of  $\beta$ -phase increases with increasing strain ratio. Higher strain ratio induces higher transformation from  $\alpha$ -phase to  $\beta$ -phase. This is similar to the conclusions given by other works about stretching of PVDF film.<sup>11</sup> However, even though higher content of  $\beta$ -phase is formed under strain ratio to 100%, the films stretched under room temperature are still mainly composed of  $\alpha$ -phase crystals.

Figure 6 gives the DSC curves of PVDF film stretched to different ratios under room temperature. After stretching to 20%, the endotherm plateau formed by annealing almost disappears. As said above, the disappearance corresponds to the formation of initial pores in the stretched samples. Also, after stretching to 20%, the weak shoulder in the annealed film disappears and the melting peak becomes narrower. Upon stretching to 60%, the maximum melting peak temperature moves to lower value. The above results indicate that the melting point of  $\beta$ -phase is less than that of  $\alpha$ -phase. With increasing strain ratio from 20 to 60%, more  $\beta$ -phase is formed. The corresponding melting peak should move to lower temperature. But this effect is very weak due to the lower content of  $\beta$ -phase. Contrary to this, the separation of main lamellae during stretching mainly induces this change. Further stretching results in the melting temperature to higher value. Although higher  $\beta$ -phase content under higher strain ratios should lead the peak temperature to lower value, some separated lamellae come together again due to the destruction of pore structure and some thicker lamellae are formed. Similar phenomenon has also been reported in the stretching of PP film to higher stretching ratio under room temperature.<sup>21</sup>

**Table II.** The Content of  $\beta$ -phase under Different Strain Ratios

Strain ratio (%)	20	40	60	80	100
$\beta$ -phase content (%)	5.4	8.6	9.8	23.5	29.7

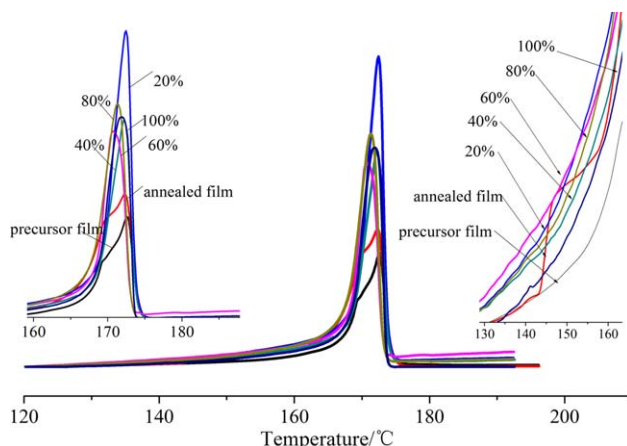


**Figure 6.** DSC curves of PVDF film stretched to different ratios under room temperature. [Color figure can be viewed in the online issue, which is available at [wileyonlinelibrary.com](http://wileyonlinelibrary.com).]

Figure 7 shows SEM of PVDF film stretched to different ratios under room temperature. For the annealed film, typical parallel lamellar structure is observed. When stretched to 20%, few pores can be seen. Further stretching to 40% initiates some pores. With increasing strain ratio to 60%, more pores can be seen. By further increasing to 80 and 100%, the distance between some separated lamellae increases, but at the same time lamellae deformation becomes apparent and some big cracks can be seen. Also some pores are closed.

As shown in Figure 7(a), the stacked lamellar crystals are formed in hard elastic PVDF film. Between the row-nucleated lamellae structure, tie chains and entanglement zones exist in the precursor film. During annealing, the tie chains directly connecting initial lamellae are included in the crystallization process, resulting in the appearance of endotherm plateau and plastic plateau in Figure 4. According to Feng,<sup>29</sup> at low temperatures, as the chain mobility was relatively low, the local stress concentration of the entanglement would be strong. Compared with the initial row-nucleated crystalline structure in the precursor film, the crystals grown around the initial lamellae during annealing from the tie chains are weak. Therefore, during the stretching in the plastic region, these crystals are first stretched and the stacked lamellae will be separated, resulting in the appearance of initial pores. After this, the stress-strain curves moves to the strain-hardening zone. During this stage, the load is transferred to the residual tie chains and the tie chains may initiate the fragmentation and tilting of lamellar crystals upon stretching. The above DSC results show that some thinner crystals among the main lamellae are torn away and reorganized into  $\beta$ -phase. This is different from the stretching process of polypropylene hard elastomer, where no crystal transformation can be observed and the stretching of some lamellae from the initial lamellae only occurs during the hot stretching process,<sup>30</sup> which forms part connecting bridges in the final microporous membrane. For PVDF, with increasing strain ratios, the transformation from  $\alpha$ -phase to  $\beta$ -phase increases, but higher deformation results in the breakage of the stacked lamellar structures.

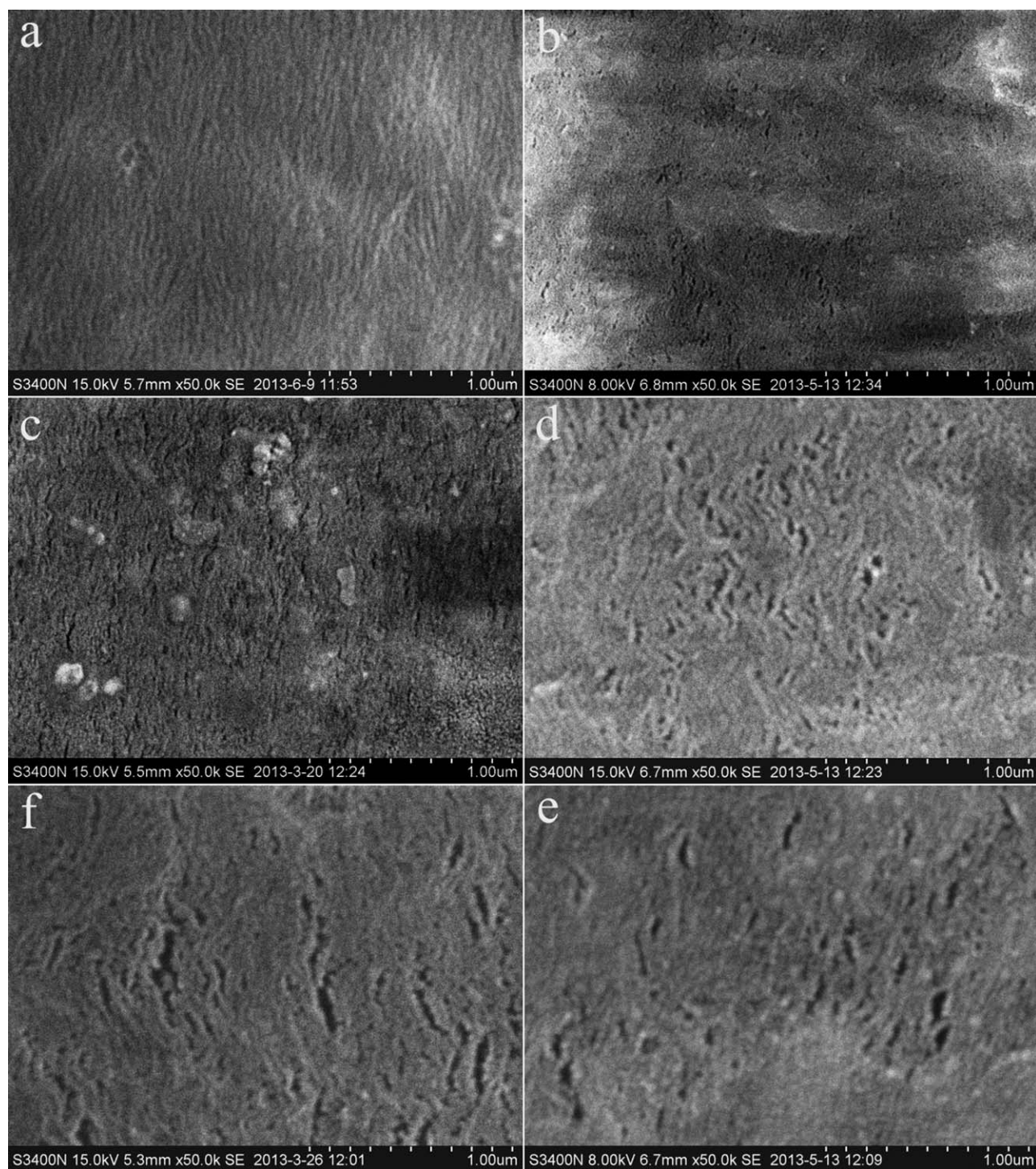


**Figure 7.** SEM of PVDF film stretched to different ratios under room temperature, (a) annealed film (b) 20% (c) 40% (d) 60% (e) 80% (f) 100%.

## CONCLUSIONS

During the room-temperature stretching of PVDF hard elastic film, strain rate and ratios show apparent influence on the crystalline morphology and microstructure. The lamellae separation, crystalline transformation from  $\alpha$ -phase to  $\beta$ -phase and the disappearance of grown crystals during annealing coexist during stretching. Under strain rate of  $0.017 \text{ s}^{-1}$  and stretching ratio

higher than 40%, better initial pore structure is obtained. But further higher strain rate and ratio lead to deformation and breakage of main lamellae structure.

## ACKNOWLEDGMENTS

The authors would like to thank National Science Foundation of Guangdong Province under Grant No. S2012010010005 and the

Provincial Department of Research Cooperation under Grant No. 2012B091100189 for financial support.

## REFERENCES

1. Khayet, M.; Feng, C. Y.; Khulbe, K. C.; Matsuura, T. *Polymer* **2002**, *43*, 3879.
2. Oshima, K. H.; Evaws-Strickfaden, T. T.; Highsmith, A. K.; Ades, E. W. *Biologicals* **1996**, *24*, 137.
3. Zukowska, G.; Rogowska, M.; Weczkowska, E.; Wieczorek, W. *Solid State Ionics* **1999**, *119*, 289.
4. Seol, W. H.; Lee, Y. M.; Park, J. K. *J. Power Source* **2006**, *163*, 247.
5. Kong, J.; Li, K. *J. Appl. Polym. Sci.* **2001**, *81*, 1643.
6. Masakazu, T.; Hitoshi, Y.; Koubc, I. Porous polyvinylidene fluoride resin film and process for producing the same. US Patent 6,299,773, **2001**.
7. Sadeghi, F.; Ajjji, A.; Carreau, P. *J. Polym. Eng. Sci.* **2007**, *47*, 1170.
8. Yu, T. H.; Wilkes, G. L. *Polymer* **1996**, *37*, 4675.
9. Du, C. H.; Xu, Y. Y.; Zhu, B. K. *J. Appl. Polym. Sci.* **2007**, *106*, 1793.
10. Sadeghi, F.; Tabatabaei, S. H.; Ajjji, A.; Carreau, P. *J. Polym. Sci. B Polym. Phys.* **2009**, *47*, 1219.
11. Salimi, A.; Yousefi, A. A. *Polym. Test.* **2003**, *22*, 699.
12. Perlman, M. M. Method to Double the Piezo- and Pyroelectric of Polyvinylidene Fluoride (PVDF) Films, US Patent 5,254,296, **1993**.
13. Gregorio, R., Jr.; Cestari, M. *J. Polym. Sci. B Polym. Phys.* **1994**, *32*, 859.
14. Andre'-Castagnet, S.; Tence'-Girault, S. *J. Macromol. Sci. Phys.* **2002**, *41*, 957.
15. Sencadas, V.; Gregorio, R., Jr.; Lanceros-Méndez, S. *J. Macromol. Sci. Phys.* **2009**, *48*, 514.
16. Mohammadi, B.; Yousefi, A. A.; Bellah, S. M. *Polym. Test.* **2007**, *26*, 42.
17. Matsushige, K.; Nagata, K.; Imada, S.; Takemura, T. *Polymer* **1980**, *21*, 1391.
18. Jing, W.; Jerold, M.; Schultz, F. Y.; Hsiao, B. S.; Benjamin, C. *Macromolecules* **2000**, *33*, 1765.
19. Johnson, M. B. Investigations of the Processing-Structure-Property Relationship of Selected Semi-crystalline Polymers. PhD Thesis, Virginia Polytechnic Institute and State University, United States, **2000**.
20. Sadeghi, F.; Ajjji, A.; Carreau, P. *J. Membr. Sci.* **2007**, *292*, 62.
21. Lei, C. H.; Huang, W. L.; Xu, R. J.; Xu, Y. Q. *J. Plast. Film Sheet* **2012**, *28*, 151.
22. Lei, C. H.; Wu, S. Q.; Xu, R. J.; Xu, Y. Q.; Peng, X. L. *Adv. Mater. Res. Int. J.* **2013**, *2*, 111.
23. Dillon, D. R.; Tenneti, K. K.; Li, C. Y.; Ko, F. K.; Sics, I.; Hsiao, B. S. *Polymer* **2006**, *47*, 1678.
24. Sobhani, H.; Razavi-Nouri, M.; Yousefi, A. A. *J. Appl. Polym. Sci.* **2007**, *104*, 89.
25. Sang-Young, L.; Soon-Yong, P.; Heon-Sik, S. *J. Appl. Polym. Sci.* **2007**, *103*, 3326.
26. Li, X. F.; Lu, X. L. *J. Appl. Polym. Sci.* **2007**, *103*, 935.
27. Du, C. H.; Zhu, B. K.; Xu, Y. Y. *J. Appl. Polym. Sci.* **2007**, *104*, 2254.
28. Satapathy, S.; Santosh, P.; Gupta, P. K.; Varma, K. B. R. *Bull. Mater. Sci.* **2011**, *34*, 727.
29. Feng, Z.; Keum, J. K.; Chen, X. M. *Polymer* **2007**, *48*, 6867.
30. Lei, C. H.; Wu, S. Q.; Xu, R. J. *Polym. Bull.* **2013**, *70*, 1353.